CRYSTAL GROWTH & DESIGN

pubs.acs.org/crystal

Article

Is the Imposition of Diamond Morphology on Mineral Inclusions a Syngenetic or Post-Genetic Process with Respect to Diamond Formation?

Marco Bruno,* Stefano Ghignone, Dino Aquilano, and Fabrizio Nestola

Cite This: *Cryst. Growth Des.* 2023, 23, 5279−5288

Read Online

ACCESS | Metrics & More | Article Recommendations | Supporting Information

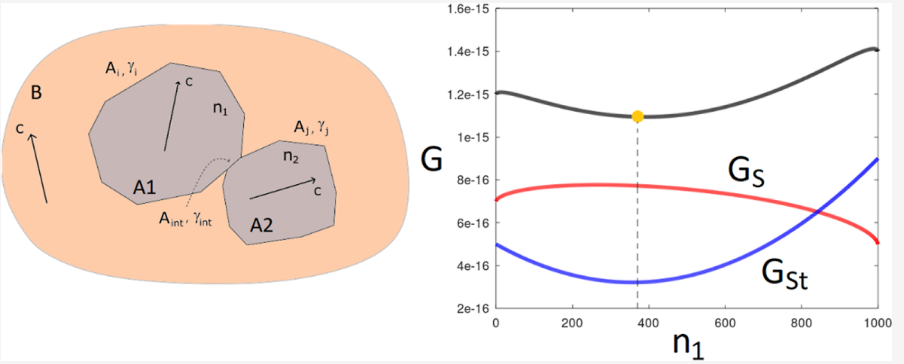

ABSTRACT: Recent studies showed that inclusions of the same phase within a single diamond are relicts of an original monocrystal that underwent a dissolution event during diamond growth. Interestingly, these inclusions developed both diamond-imposed (i.e., cubic-octahedral shape) and lobed morphologies with rounded shapes and/or embayments. Whether the diamond-imposed morphology is developed during or after entrapment of the inclusion is unknown. We addressed the problem in two ways: (i) by determining the thermodynamic conditions under which mineral inclusions can modify their size (e.g., a single inclusion separates to give two inclusions with different size) and morphology, when trapped in diamond and (ii) by critically reviewing and discussing the recent observations on mineral inclusions in diamond. Accordingly, we developed a thermodynamic model which considers all the involved energetic contributions (i.e., surface and strain energies) to completely describe the Gibbs energy of a closed system designed to forecast the size evolution of two adjacent (or a single) inclusions, at constant T and P. Based on this model and analyzing the existing scientific literature on diamond, we propose an experimental/observational protocol to evaluate whether post-entrapment modification of inclusions has occurred.

1. INTRODUCTION

Inclusions in diamond (hereafter DIs) have been classified according to the timing of their formation related to the host diamond:[1−3] syngenetic inclusions were formed at the same time and from the same chemical reaction that produced the diamond; protogenetic inclusions represent pre-existing materials that were passively incorporated into the growing diamond; and epigenetic inclusions are materials crystallized after diamond formation, as exhaustively detailed by Nestola et al.:[4]

(i) syngenesis implies simultaneous growth of both inclusion and host, as a result of co-precipitation from the same medium. Complete re-crystallization of a pre-existing mineral (e.g., by a dissolution/re-precipitation process) simultaneously with the diamond growth may also allow for co-precipitation and, therefore, syngenesis. In both cases, the inclusion should presumably be in equilibrium with the diamond-forming medium.

(ii) Conversely, a protogenetic inclusion may only re-equilibrate with the diamond-forming medium through intra-crystalline diffusion before its encapsulation, and its composition may or may not be fully reset during diamond formation. Therefore, chemical equilibrium of an inclusion with the diamond-forming medium would rarely occur and would not necessarily imply syngenesis.

To identify syngenetic inclusions is of paramount importance in diamond studies. Since diamond behaves as an inert container, any geological information extracted from a syngenetic inclusion (e.g., pressure and temperature of

Received: April 18, 2023
Revised: June 5, 2023
Published: June 16, 2023

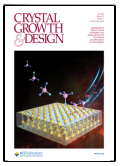

https://doi.org/10.1021/acs.cgd.3c00474
Cryst. Growth Des. 2023, 23, 5279−5288

formation, age, and geochemistry of the parent medium) should also unequivocally apply to its host diamond. Currently, there are no criteria that unambiguously allow classifying a mineral inclusion in diamond as proto- or syngenetic. Some criteria have been proposed in the past, but they are not based on well-grounded physicochemical bases, but on some beliefs or erroneous interpretations concerning crystal growth phenomena.

The most common used potential indicators of syngenesis are: (i) diamond imposes its morphology on the inclusion[1,5−10] and (ii) epitaxial relationships between the inclusion and its host.[6,7,9−11] Interestingly, such criteria are adopted to discriminate between proto- and syngenetic inclusions in diamond, but they have never been considered when studying mineral inclusions in, for example, metamorphic garnets. The inclusions are usually considered syngenetic with the garnet, and it is assumed that the different growth zones of the garnet (i.e., core and rim) encapsulate a mineralogical paragenesis developing contemporaneously. The alternative situation that some minerals are pre-existing (protogenetic) and, therefore, were only partially reabsorbed before being incorporated into the garnet is rarely evaluated. Indeed, the extensive use of pseudo-sections to reproduce mineralogical parageneses embedded in garnet for constraining $P-T$ conditions encountered by the host rock, is based on the hypothesis of syngenesis.

Criterion (i) is based on the belief that diamond can impose its morphology upon the inclusion only during latter's growth, owing to diamond's much greater formation energy,[7] also named crystalloblastic force of diamond faces. An ill-defined force is invoked to explain the morphology of the inclusions, a force whose origin does not exist in crystal growth theory, the relevance of which is not absolutely clear. This criterion was initially challenged by Taylor et al.[12,13] and subsequently by Nestola et al.[4] In particular, by measuring the crystallographic orientations of numerous olivine inclusions in diamond with imposed morphology, Nestola et al.[4] were able to establish their protogenetic origin; the same approach was also applied to garnet and pyroxene inclusions.[14,15] Hence, this criterion has been refuted: the discovery of protogenetic inclusions with diamond-imposed morphology contradicts the initial hypothesis. This does not mean that all inclusions with diamond-imposed morphology are protogenetic, but it simply means that this criterion is no longer applicable to discriminate unequivocally between syngenesis and protogenesis.

A post-entrapment shape maturation process was recently proposed by Cesare et al.[16] to explain the morphology of quartz inclusions in garnet of high-T rocks under granulite-facies conditions. They observed that in granulite-facies samples from high-T (>750 °C) rocks, quartz inclusions (10−100 μm in size) in garnet systematically show a polyhedral shape controlled by the surrounding host. Moreover, Cesare et al.[16] observed that quartz inclusions in the greenschist-facies low-T (<550 °C) samples are frequently larger in size (up to 150 μm) and exhibit anhedral shape. These quartz inclusions have a large surface/volume ratio (S/V) when compared to high-T faceted inclusions with similar volumes. These distinct differences between quartz inclusions in high and low-T samples, along with the observed high-T samples containing numerous examples of pinch-and-swell-like pairs or groups of inclusions in contact along small and often cuspate necks, suggested to the authors that the shape maturation of quartz inclusions takes place in garnets at high-T, analogous to the process occurring in fluid and melt inclusions. In particular, these microstructures show strong similarities with geometries developed by the process of necking down of fluid inclusions[17] and in ceramics (de-sintering process):[18] polycrystalline aggregates break into isolated grains through the formation of a connecting thin channel allowing exchange of matter.

According to these findings, Cesare et al.[16] proposed that, at high-T, quartz inclusions originally in contact can suffer shape maturation by thermally activated grain-boundary diffusion along dry interphase boundaries,[19] to the point of separating and generating a crystalline habit, which reflects that of the host garnet. If this does occur, the system could approach equilibrium by increasing the S/V ratio, which opposes what is usually expected, that is, coarsening by crystal coalescence to minimize the surface free energies and reduce the S/V ratio.

Thus, Cesare et al.[16] proposed that the imposed morphology is not due to syngenesis, but developed subsequent to the entrapment of the inclusion. This could highlight further that the morphological criterion cannot be applied to establish syngenesis.

Here, we will try to answer if the post-entrapment shape maturation process is thermodynamically possible, and if the diamond-imposed morphology can be an effect of this by (i) determining the thermodynamic conditions for which two inclusions originally in contact (or one inclusion) can separate and modify their shapes after trapping and (ii) critically reviewing and discussing the recent observations on the inclusions in diamond.

2. THERMODYNAMIC MODEL

We have built a true physical thermodynamic model by considering all the involved energetic contributions to completely describe the Gibbs energy of a closed system composed of two mineral inclusions trapped in a host phase; the model is also designed to describe the evolution of a single inclusion, i.e., its eventual separation into two individuals and/or its shape evolution. Moreover, the model is valid for any inclusion-host pair. As we will see, the mere consideration of the surface energies in the Gibbs energy minimization of the system cannot lead to separation of the inclusions. To correctly describe the evolution of the system, it is necessary to introduce an additional term representing the strain energy of the inclusion due to the stress imposed by the host. Minerals trapped as inclusions at $[T_0, P_0]$ within a host mineral can develop residual stresses when pressure and temperature are changed to $[T \neq T_0, P \neq P_0]$, because of the differences between the thermo-elastic properties (i.e., thermal expansion and compressibility) of the host and inclusion phases.[20−23] We will show that, at constant temperature and pressure when the strain energy exceeds a threshold value, the minimum of the Gibbs energy is reached by separating the two inclusions originally in contact, thus increasing the S/V ratio. The model we propose makes use of several approximations, but despite everything, offers the advantage of describing the equilibrium of the system under different conditions and thermodynamically explains when the inclusions can coalesce or separate.

It is also worth underlining that this model cannot describe the kinetics of the transformation, but only allows for determination of the amount of matter of each inclusion at equilibrium. Additionally, we discuss some considerations about the kinetics of the post-entrapment modification mechanism to describe the evolution of the inclusion-host

https://doi.org/10.1021/acs.cgd.3c00474
Cryst. Growth Des. 2023, 23, 5279−5288

system, in order to establish if the post-entrapment mechanism hypothesized for quartz inclusions in garnet can be applicable for inclusions in diamond.

Within this model, we assume two crystals of phase A in contact, A1 and A2, hosted in phase B (Figure 1). A1 and A2

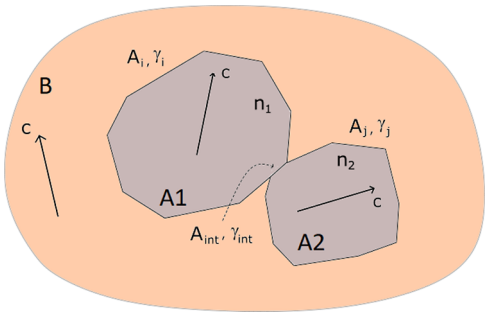

Figure 1. Schematic diagram representing two mineral inclusions (A1 and A2) trapped in the host phase (B) at T_0 and P_0. Black arrows indicate the crystallographic orientations of the c axis of the crystals. In this diagram, two inclusions (A1 and A2) with different crystallographic orientations are illustrated, while the case of the two inclusions having the same orientation is also discussed in the main text.

are composed of n_1 and n_2 formula units (f.u.), respectively. Moreover, A1 and A2 are oriented differently from each other and also with respect to B; crystal orientations are exemplified in Figure 1 by their crystallographic $\boldsymbol{c}$ axes.

A1 and A2 were trapped in phase B during growth at given temperature and pressure, T_0 and P_0. The system A + B experiences $T \neq T_0$ and $P \neq P_0$ variations post-formation. Thus, how do the quantities n_1 and n_2 change at the new T and P, once equilibrium is reached? Hence, we must determine the values of n_1 and n_2 at $T \neq T_0$ and $P \neq P_0$ (i.e., the equilibrium size of the two inclusions in contact, A1 and A2). A variation of n_1 and n_2 should imply a modification of each inclusion's volumes and, probably, of their shapes.

To give an answer, we need to evaluate the minimum of the Gibbs energy (G) of the closed system A + B at T, P, and $N = n_B + n_1 + n_2$ constants, with n_B being the number of f.u. in phase B. The Gibbs energy of the system at given T, P, and N reads

$$G(T, P, N) = \mu_B n_B + \mu_A(n_1 + n_2) + \sum_i^{A1} \gamma_i A_i + \sum_j^{A2} \gamma_j A_j + \gamma_{int} A_{int} + \Phi_{A1} V_{A1} + \Phi_{A2} V_{A2} \quad (1)$$

where μ_B and μ_A are the chemical potentials (J/f.u.) of phases B and A at T and P, while γ_i and γ_j are the energies (J/m^2) of the i-th and j-th interfaces, defining the contacts B/A1 and B/A2 (Figure 1); γ_{int} is the energy (J/m^2) of the A1/A2 interface, while A_i, A_j, and A_{int} are the areas (m^2) of the interfaces B/A1, B/A2, and A1/A2; finally, Φ_{A1} and Φ_{A2} are the strain energies per unit volume (J/m^3) of A1 and A2, and V_{A1} and V_{A2} represent their volumes (m^3).

If the inclusion is considered isotropic, it will also have isotropic compressibility, and therefore, will exhibit equal stresses in all directions; the normal stresses in any three perpendicular directions will be equal, and the inclusion will be subject to a hydrostatic pressure.[24] As discussed by Angel et al.,[25] this assumption is reasonable when studying DIs. Moreover, 68% of all reported DIs are composed of two cubic minerals (garnet and Mg-chromite) and an orthorhombic one (olivine),[26] the latter showing hydrostatic behavior when included in diamond.[27]

Equation 1 can be rewritten as follows

$$G(T, P, N) = G_V + G_S + G_{St} \quad (2)$$

where G_V, G_S, and G_{St} are the Gibbs energies of volume, surface, and strain, respectively

$$G_V = \mu_B n_B + \mu_A(n_1 + n_2) \quad (3)$$

$$G_S = \sum_i^{A1} \gamma_i A_i + \sum_j^{A2} \gamma_j A_j + \gamma_{int} A_{int} \quad (4)$$

$$G_{St} = \Phi_{A1} V_{A1} + \Phi_{A2} V_{A2} \quad (5)$$

In closed systems, the term G_V does not undergo variations if T, P, n_B, and $n_1 + n_2 = n$ are held constant. Therefore, term G_V will be not considered in our analysis, since it remains constant, as n_1 and n_2 vary during the reshaping of the inclusions A1 and A2, but $n_1 + n_2$ = const. Indeed, the first derivative of eq 2, calculated to find the minimum of function G, is not affected by term G_V, which is a constant, its derivative being equal to zero.

We can further simplify eq 1 by supposing that A_{int} is negligible with respect to A_i and A_j. This implies that the inclusions A1 and A2 are in contact through a very small area of the A1/A2 interface (Figure 1). Then, $\gamma_{int} A_{int} \approx 0$.

Now, we can express A_i and A_j as a function of n_1 and n_2 by means of the shape coefficients c_i and c_j, respectively:[28] $A_i = c_i n_1^{2/3}$ and $A_j = c_j n_2^{2/3}$. Similarly, we can express the volumes of the inclusions as: $V_{A1} = \Omega n_1$ and $V_{A2} = \Omega n_2$, with Ω being the volume of a f.u. (m^3/f.u.) of the phase A. Finally, by using the relation $n_2 = n - n_1$, eq 1 can be written through n_1 and reads

$$G(T, P, n_1) = n_1^{2/3} \sum_i^{A1} \gamma_i c_i + (n - n_1)^{2/3} \sum_j^{A2} \gamma_j c_j + \Phi_{A1} \Omega n_1 + \Phi_{A2} \Omega (n - n_1) \quad (6)$$

2.1. Simplifications of Our Model. Equation 6 can be further simplified without altering the physical constraints of the model. The inclusions with different orientations with respect to the hosting mineral have a different average interfacial energy, regardless of their equilibrium shape, according to the Gibbs–Wulff theorem that describes the equilibrium morphology of a crystal.[28] Then, we can use the following relations

$$\sum_i^{A1} \gamma_i c_i \approx \langle \gamma \rangle_{A1} \sum_i c_i \quad (7)$$

$$\sum_j^{A2} \gamma_j c_j \approx \langle \gamma \rangle_{A2} \sum_j c_j \quad (8)$$

where $\langle \gamma \rangle_{A1}$ and $\langle \gamma \rangle_{A2}$ are the weighted mean interfacial energies. If one approximates that all the shape coefficients are equal, $c_i = c_j = c$ (see the Supporting Information for the calculation of the shape coefficient), we can write

https://doi.org/10.1021/acs.cgd.3c00474
Cryst. Growth Des. 2023, 23, 5279−5288

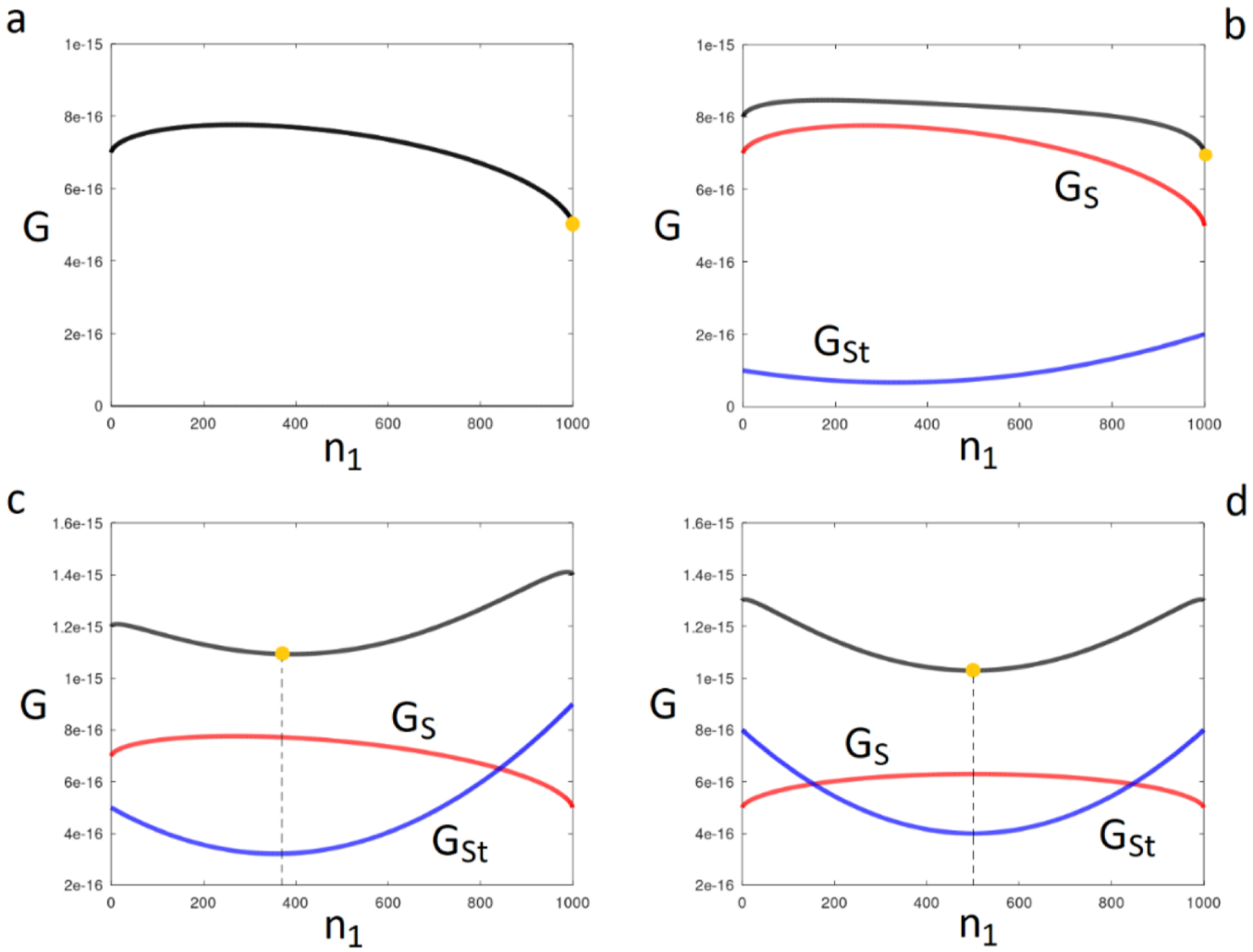

Figure 2. Gibbs energy (J) of the system as a function of n_1 for different values of the parameters: (a) non-stressed inclusions differently oriented ($\varepsilon_{Ol1} = \varepsilon_{Ol2} = 0$; $\langle\gamma\rangle_{Ol1} = 5.0$ J/m^2 and $\langle\gamma\rangle_{Ol2} = 7.0$ J/m^2); (b) slightly stressed inclusions differently oriented ($\varepsilon_{Ol1} = 2.797 \times 10^6$ J/(f.u. m^3) and $\varepsilon_{Ol2} = 1.399 \times 10^6$ J/(f.u. m^3); $\langle\gamma\rangle_{Ol1} = 5.0$ J/m^2 and $\langle\gamma\rangle_{Ol2} = 7.0$ J/m^2); (c) strongly stressed inclusions differently oriented ($\varepsilon_{Ol1} = 1.259 \times 10^7$ J/(f.u. m^3) and $\varepsilon_{Ol2} = 6.993 \times 10^6$ J/(f.u. m^3); $\langle\gamma\rangle_{Ol1} = 5.0$ J/m^2 and $\langle\gamma\rangle_{Ol2} = 7.0$ J/m^2); (d) strongly stressed inclusions equally oriented ($\varepsilon_{Ol1} = \varepsilon_{Ol2} = 1.119 \times 10^7$; $\langle\gamma\rangle_{Ol1} = \langle\gamma\rangle_{Ol2} = 5.0$ J/m^2). Solid yellow circle indicates the minimum of the Gibbs energy.

$$\langle\gamma\rangle_{A1}\sum_i c_i \approx cr\langle\gamma\rangle_{A1} \tag{9}$$

$$\langle\gamma\rangle_{A2}\sum_j c_j \approx cl\langle\gamma\rangle_{A2} \tag{10}$$

where r and l are the whole number of the i-th and j-th interfaces, respectively. Finally, eq 6 becomes

$$G(T, P, n_1) = cr\langle\gamma\rangle_{A1} n_1^{2/3} + cl\langle\gamma\rangle_{A2}(n - n_1)^{2/3} + \Phi_{A1}\Omega n_1 + \Phi_{A2}\Omega(n - n_1) \tag{11}$$

In what follows, we consider $cr\langle\gamma\rangle_{A1}$ and $cl\langle\gamma\rangle_{A2}$ as constants, considering that the inclusion shapes do not change with size (i.e., we assume a homothetic variation). Two cases are then discussed:

(i) two chemically identical inclusions having different orientations. To model this case, we set $cr\langle\gamma\rangle_{A1} \neq cl\langle\gamma\rangle_{A2}$, as the interfaces A1/B and A2/B are different.

(ii) Two chemically identical inclusions having equal crystallographic orientation. Since at equilibrium, they must develop the same crystal morphology according to the Gibbs–Wulff theorem,[28] this condition is described by setting $cr\langle\gamma\rangle_{A1} = cl\langle\gamma\rangle_{A2}$.

Hence, the quantities Φ_{A1} and Φ_{A2} remain to be discussed. According to the classic elastic theory,[24] Φ_{A1} and Φ_{A2} depend exclusively on the reciprocal orientation between inclusions and host mineral, since they are independent of the size of the inclusion (i.e., on n_1 or n_2). This implies that G_{St} is linear with respect to n_1. Consequently, eq 11 can only have minima when $n_1 = 0$ and/or $n_1 = n$, and the coexistence of two inclusions with different (or equal) size (i.e., $n_1 \neq 0$) is not allowed. Such coexistence can only occur when Φ_{A1} and Φ_{A2} are supposed to be also a function of the inclusion size, in contrast to the classic elastic theory; a detailed discussion is reported in the Supporting Information. Therefore, we use the following relationships to describe the dependence on the size of the functions Φ_{A1} and Φ_{A2}

$$\Phi_{A1} = \varepsilon_{A1} n_1 \tag{12}$$

$$\Phi_{A2} = \varepsilon_{A2} n_2 = \varepsilon_{A2}(n - n_1) \tag{13}$$

where ε_{A1} and ε_{A2} are constants, J/(f.u. m^3), their values depending also on the orientation of inclusion A with respect

https://doi.org/10.1021/acs.cgd.3c00474
Cryst. Growth Des. 2023, 23, 5279−5288

to host phase B. Thus, two equally oriented inclusions must have $\varepsilon_{A1} = \varepsilon_{A2}$. With increase of the inclusion's volume, Φ_{A1} (Φ_{A2}) linearly increases as a function of n_1 (n_2). Finally, by inserting eqs 12 and 13 in eq 11, one obtains

$$G(T, P, n_1) = cr\langle\gamma\rangle_{A1} n_1^{2/3} + cl\langle\gamma\rangle_{A2}(n - n_1)^{2/3} + \varepsilon_{A1}\Omega n_1^2 + \varepsilon_{A2}\Omega(n - n_1)^2 \quad (14)$$

used to discuss the evolution of the inclusions (next paragraph). Now, G_S and G_{St} read

$$G_S = cr\langle\gamma\rangle_{A1} n_1^{2/3} + cl\langle\gamma\rangle_{A2}(n - n_1)^{2/3} \quad (15)$$

$$G_{St} = \varepsilon_{A1}\Omega n_1^2 + \varepsilon_{A2}\Omega(n - n_1)^2 \quad (16)$$

where their relative weight influences the equilibrium conditions of our system. Now, G_{St} is a quadratic function with respect to n_1, with the concavity pointing up (see Supporting Information).

3. DISCUSSION OF THE MODEL AND COMPARISON WITH PREVIOUS MODELS

Now, we aim at discussing our thermodynamic model for two olivine inclusions (A1 = Ol1 and A2 = Ol2) in diamond (B = D); however, this model can be applied to the study of any mineral inclusion/host. Bruno et al.[29] calculated at a quantum-mechanical level the interfacial energies (J/m^2) of some D/Ol interfaces: $\gamma_{(001)_D/(001)_{Ol}} = 6.105$, $\gamma_{(001)_D/(021)_{Ol}} = 6.477$, $\gamma_{(111)_D/(001)_{Ol}} = 6.459$, and $\gamma_{(110)_D/(101)_{Ol}} = 6.375$. Therefore, in what follows, we consider that the averaged values of $\langle\gamma\rangle_{Ol1}$ and $\langle\gamma\rangle_{Ol2}$ are of the same order of magnitude to those estimated by Bruno et al.[29] Then, we determine the minimum of the Gibbs energy of the system from eq 14 by considering different conditions: from the strain energy equal to zero (i.e., stress-free inclusions, $G_{St} = 0$) to strain energy values giving G_{St} comparable to G_S. The aim of these calculations is to evaluate the different behavior of the system when the G_{St}/G_S ratio changes. We want to emphasize here that it is not our intention to provide realistic estimates of the energy contributions introduced in the thermodynamic model. In this work, we limit the evaluation to how the equilibrium changes between two inclusions in contact, when varying the G_{St}/G_S ratio. However, in all these cases, we fix: (i) $\Omega = 7.15 \times 10^{-29}$ m^3/f.u., (ii) $c = 10^{-19}$ m^2, (iii) $r = l = 10$, and (iv) $n = 1000$. The choice of the values of r, l, and n is completely arbitrary, as the results of our model depend exclusively on the G_{St}/G_S ratio.

3.1. Stress-free Inclusions. In the simplest case, two adjacent non-stressed trapped olivine inclusions follow $\Phi_{Ol1} = \Phi_{Ol2} = 0$. Equation 14 reduces to single term G_S (eq 15), being $G_{St} = 0$.

By using $\langle\gamma\rangle_{Ol1} = 5.0$ J/m^2 and $\langle\gamma\rangle_{Ol2} = 7.0$ J/m^2, which implies that the inclusions have different orientations, we report $G = G_S$ as a function of n_1 in Figure 2a. The lowest value of G occurs at $n_1 = 1000$: two non-stressed inclusions cannot coexist at the equilibrium, and the one with the highest average surface energy (Ol2) disappearing in favor of that with the lowest average surface energy (Ol1), in order to reduce the S/V ratio.

The same behavior should occur for two equally oriented inclusions, $\langle\gamma\rangle_{Ol1} = \langle\gamma\rangle_{Ol2}$: in fact, G has two identical minima at $n_1 = 1000$ and $n_1 = 0$ ($n_2 = 1000$); and one out of the two inclusions must disappear in favor of the other one.

3.2. Stressed Inclusions. When two stressed inclusions are in contact with different crystallographic orientations, it holds: $\Phi_{Ol1} \neq \Phi_{Ol2} \neq 0$. Considering again $\langle\gamma\rangle_{Ol1} = 5.0$ J/m^2 and $\langle\gamma\rangle_{Ol2} = 7.0$ J/m^2, and according to the amount of strain energy stored up in the inclusions, two cases can be envisaged:

(i) The strain energy, J/(f.u. m^3), is low (e.g., $\varepsilon_{Ol1} = 2.797 \times 10^6$ and $\varepsilon_{Ol2} = 1.399 \times 10^6$): the minimum of G is always at $n_1 = 1000$ (Figure 2b); as in the previous case, to reduce the S/V ratio, the inclusion having the highest average surface energy value (Ol2) would disappear in favor of that with the lowest energy (Ol1).

(ii) The strain energy is high (e.g., $\varepsilon_{Ol1} = 1.259 \times 10^7$ and $\varepsilon_{Ol2} = 6.993 \times 10^6$): the minimum of G is for $n_1 \sim 350$ (Figure 2c). Here, the equilibrium is obtained when the two inclusions have different sizes. When strain energy exceeds a threshold value, equilibrium takes place when the S/V ratio increases. The n_1/n_2 ratio at the equilibrium depends on the relative weight of the different energetic contributions describing the function G, i.e., G_S and G_{St}. Stressed olivine inclusions can reduce their Gibbs energy by increasing the S/V ratio.

Instead, when two strongly stressed inclusions have equal orientation, $\langle\gamma\rangle_{Ol1} = \langle\gamma\rangle_{Ol2} = 5.0$ J/m^2 and $\varepsilon_{Ol1} = \varepsilon_{Ol2} = 1.119 \times 10^7$ J/(f.u. m^3), the minimum of G is attained at $n_1 = n_2 = 500$ (Figure 2d). At equilibrium, two inclusions with equal size and shape must coexist. Interestingly, the same parameters describe the evolution of a single strongly stressed inclusion, having supposed in our model that $\gamma_{int}A_{int} \approx 0$. Indeed, this relation is valid when either $A_{int} = 0$ or $\gamma_{int} = 0$. However, $\gamma_{int} = 0$ means that there is not an interface between the two crystals in contact: then, we are dealing with a single crystal. When a large inclusion is strongly stressed, two (or more) individuals with equal and reduced size become stable: according to our model, smaller inclusions have G_{St} values lower than a single large inclusion.

Our model was designed to study the size evolution of two mineral inclusions in contact. The separation of two inclusions from an original single one could occur when, from an energetic point of view, it is favorable to replace the single interface Ol1/Ol2 (Figure 1) with two interfaces Ol1/D and Ol2/D such as $\gamma_{int}A_{int} > \gamma_{Ol1/D}A_{Ol1/D} + \gamma_{Ol2/D}A_{Ol2/D}$. If this condition is satisfied, along with that described in the preceding point (ii), then the separation of the inclusions is thermodynamically allowed. After the separation of the two inclusions, their crystal forms can evolve until equilibrium is reached, their morphology being ruled by the Gibbs–Wulff theorem[28]

$$\frac{\gamma_1}{h_1} = \frac{\gamma_2}{h_2} = \ldots = \frac{\gamma_i}{h_i} = \text{const} \quad (17)$$

which states that, at the equilibrium, the ratio between the interfacial energy (γ_i) of i-th interface Ol/D and the distance of the same interface from the crystal's barycenter (h_i) is a constant. Equation 17 comes when minimizing the sum $\sum_i \gamma_i A_i$, at constant volume. Such a theorem could explain the polyhedral shape of the olivine and quartz inclusions that mimics that of the diamond and garnet host, respectively. The system "inclusion/host" tends to reduce its Gibbs energy by generating the interfaces which allow attaining the minimum of the quantity $\sum_i \gamma_i A_i$. It is worth remembering that in eq 17 the constant value is not uncertain, but const = $\Delta\mu/2\Omega$,[28] where

https://doi.org/10.1021/acs.cgd.3c00474
Cryst. Growth Des. 2023, 23, 5279−5288

$\Delta\mu$ and Ω represent the thermodynamic supersaturation and the molecular volume, respectively, of each described crystal phase.

3.3. Previous Thermodynamic Models. To the best of our knowledge, there are no adequately developed thermodynamic models to explain the evolution of two adjacent minerals included in a crystalline host. As briefly mentioned in the Introduction, the microstructures observed in the rocks by Cesare et al.[16] reflect those in ceramics when a de-sintering process has occurred.[18] De-sintering is a common phenomenon occurring in partially dense bodies, where polycrystalline aggregates (e.g., fibers) break into isolated grains.

Miller and Lange[30] explained the breaking of fibers in isolated spherical crystals by considering only the effect of surface and interface energies on the Gibbs function; no considerations about the crystal's orientation and strain energy were developed. The initial structure of the fiber is modeled by using identical cylindrical grains (e.g., same length and diameter). Moreover, it was assumed that the grain centers are constrained to stay at a fixed distance, each grain retaining its initial mass. Therefore, the constraints imposed in this model force the fibers to separate into single crystals that are able to lower the Gibbs energy. In any case, this model does not allow formation of a single crystal starting from two crystals.

Progressive shape evolution of a mineral inclusion under differential stress at high temperature was modeled by Okamoto and Michibayashi.[31] These authors predicted the progressive change in the aspect ratio of a single ellipsoidal inclusion (garnet) within a host mineral (quartz) by means of an analytical model considering both dislocation and interface diffusion creep, and rounding by interface diffusion. In their model, it was assumed that the garnet/quartz interface free energy is independent of the crystallographic orientation, and an interface energy of 1 J/m^2 was used. This is a very interesting model to evaluate the stress effect on the shape modification of a single inclusion, but it was not developed to analyze the behavior of multiple adjacent inclusions.

3.4. Some Considerations on Growth Kinetics. During the separation of the inclusions and their shape evolution, there is significant mass transfer, both from the host and inclusions. This must occur at constant volume by means of growth/dissolution processes occurring at the host/inclusion interface, coupled with grain boundary diffusion: a given volume increase of an inclusion must be accompanied by the same volume reduction of the other one. The system evolves to equilibrium only via the progressive reduction of the Gibbs energy, due to the matter transfer from one inclusion to another. For two inclusions to reach their equilibrium size, it is mandatory that they remain in contact at least for the time necessary for the transfer of matter suitable to the purpose, since any premature separation of the two inclusions would hinder the achievement of the equilibrium size. Once the transfer of matter is completed, the inclusions separate and readjust their shape, thereby reducing the interfacial energy and developing their equilibrium morphology. Therefore, the stage of necking down is mandatory to create a bridge for exchanging matter among the inclusions. For this process to occur, high temperatures are needed to favor grain-boundary diffusion along the host/inclusion interfaces.

4. SOME OBSERVATIONS ON INCLUSIONS IN DIAMOND

DIs show both imposed-morphology and lobed morphology, i.e., crystals with rounded shape and/or embayments. Such lobed morphology is usually considered as evidence of resorption phenomena, although recently this peculiar shape has been associated with the necking down process previously discussed.[16] Re-evaluating literature DI observations can determine if necking down is a realistic process in diamonds. Here we summarize the DI observations from the scientific literature:

(i) Within a single diamond, it is possible to find several inclusions of the same phase (e.g., olivine) having equal crystallographic orientation (but different orientations with respect to the diamond host); these inclusions were interpreted by Nestola et al.[4] as relicts of an original single monocrystal that underwent dissolution during diamond growth. Then, regardless of the possible chemical re-equilibration during diamond-forming processes, these inclusions have existed prior to the diamond (i.e., they are protogenetic). This interpretation was subsequently strengthened by the discovery in a xenolith of a clinopyroxene (external to diamond) with the same composition and crystal orientation of the clinopyroxene relicts included in the diamond (again, this orientation was different from that of the diamond host).[32] Subsequently, Nimis et al.[33] documented two iso-oriented inclusions of magnesiochromite, which clearly are the remains of an original single crystal partially resorbed during the diamond growth, highlighting the protogenetic character of the iso-oriented inclusions.

(ii) In all the papers reporting crystal orientation relationships between inclusions and diamonds, at most three distinct sets of similarly oriented inclusions have been found within a single diamond.[4,5,7,10,11,14,15,33−42]

(iii) Iso-oriented protogenetic inclusions show both a diamond-imposed morphology [e.g., olivine with (pseudo) cubo-octahedral morphology] and a lobed morphology.[4,14] The coexistence of these two different morphologies in the same diamond can inform us about the variation of the diamond growth rate during its formation history. However, as discussed later, this information can only be extracted when the diamond growth zonation is known.

(iv) By performing micro-Raman spectroscopy on DIs, Nimis et al.[43] found that typical mineral inclusions in diamonds from the Siberian and Kaapvaal cratons are surrounded by a film of hydrous silicic fluid having a maximum thickness of 1.5 μm. The same fluid was later detected by Nestola et al.[44] During diamond growth, such a fluid could act as an interface diffusion medium enabling the selective dissolution of pre-existing minerals to create the diamond-imposed shapes of many inclusions.

(v) In almost all the reported studies on DIs, there are no detailed analyses on: (a) the morphology/size relation of inclusions (i.e., are inclusions with diamond-imposed morphology larger than those with lobed morphology?) and (b) the location of inclusions in the diamond (i.e., are inclusions located at the diamond center or in the periphery?)

https://doi.org/10.1021/acs.cgd.3c00474
Cryst. Growth Des. 2023, 23, 5279−5288

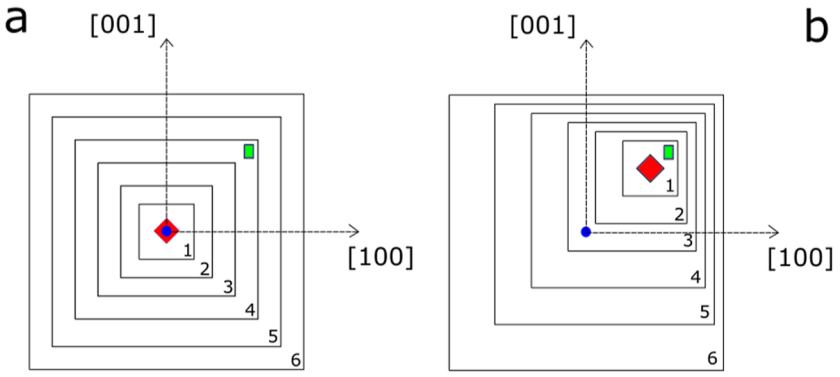

Figure 3. Schematic image representing the (a) homothetic and (b) nonhomothetic growth of a diamond: blue circle and red square represent the barycenter and central growth zone of the diamond respectively; the green rectangle is a mineral inclusion; the diamond growth zones around the central one, are numbered from 1 to 6.

The coexistence of iso-oriented inclusions with both imposed and lobed morphologies in the same diamond suggests the following two possible hypotheses if we assume that they come from a single resorbed original crystal:

(i) The shape of the inclusion is not modified, once trapped in the diamond. Then, the different inclusion morphologies are the consequence of the growth and dissolution rates of the diamond and mineral undergoing resorption, respectively. It is likely that a low diamond growth combined with a low dissolution rate of the reabsorbed mineral favors the development of inclusions with diamond-imposed morphology to minimize the energy of the system, generating inclusion/diamond interfaces having the lowest possible interfacial energies. Conversely, both high diamond growth rate and high inclusion dissolution rate do not allow for readjustment of the inclusion/diamond interfaces; thus, it is reasonable to expect crystals with lobed morphology.

(ii) The inclusion shape can change, once trapped in the diamond, by means of thermally activated grain-boundary diffusion along dry (or wet) interphase boundaries, generating a crystal habit which reflects that of the host diamond. If this can occur, then the discovery of inclusions with both imposed and lobed morphology means that the shape maturation process has involved only some relicts of the partly resorbed single crystal. This can only happen when the inclusions have been trapped at different times: the first to be incorporated into the diamond will be those that have had more time to adjust their morphology. On these grounds, inclusions with imposed morphology should lie closer to the central growth zone of the diamond than those with lobed morphology. Therefore, it is crucial to associate the mineral inclusions with the respective growth sectors of the diamond, to disprove or validate the post-entrapment shape maturation process.

In this light, it is evident that a correct analysis of the two possible processes requires determination of the position of the inclusions inside the diamond: are they near the barycenter, i.e., in an intermediate position, or in the periphery of the diamond? Nevertheless, these data can be misleading when they are not associated to specific growth zonations observed by cathodoluminescence (CL).[39,45−51] Indeed, only when diamond grows homothetically (i.e., equivalent faces advance with the same rate), the barycenter of the crystal (blue circle in Figure 3a) coincides with the central growth zone of the diamond (red square in Figure 3a). When the growth is not homothetic, then the central growth zone of the diamond no longer coincides with the gravity-center of the crystal (Figure 3b). This concept is clearly illustrated in Figure 3, where two diamonds with the same size and morphology can register a completely different growth history. Here we specify two hypothetical cases:

(i) the diamond is grown homothetically, then the inclusion is also peripheral with respect to the central growth zone (growth zone 4, Figure 3a);

(ii) the diamond is not grown homothetically, then the inclusion can be in proximity of the central growth zone (growth zone 1, Figure 3b).

It follows that the interpretations on the genesis of the inclusion can be different according to its positioning with respect to the effective growth center of the diamond. Moreover, an inclusion lying far from the barycenter of the diamond could nonetheless have served as a substrate for diamond nucleation, since it could actually be located in the central growth zone of the diamond.

4.1. Strategy to Evaluate the Existence of Post-Entrapment Modification. A reasonable way to evaluate whether the post-entrapment modification can occur is the following:

(i) Finding a diamond (or garnet) host having two or more mineral inclusions with the same crystallographic orientation and exhibiting both diamond- (or garnet)-imposed and lobed morphology; the same orientation guarantees that the inclusions are relicts of an original monocrystal. The crystallographic orientations of the inclusions in diamond can be determined either by single-crystal X-ray diffraction, or by means of electron backscatter diffraction (EBSD) for those inclusions lying inside the garnet.

(ii) Determining the position of the inclusions with respect to the diamond (or garnet) growth sectors. Such sectors can be observed in diamond by means of cathodoluminescence (CL), while for the garnet, they can be easily visualized by compositional maps obtained with electron microprobe analysis (EMPA).

(iii) Two cases can be imagined: (1) inclusions with imposed morphology are located closer to the central growth zone of the diamond (or garnet) than those with lobed morphology (Figure 4a). In this case, it is not possible to

https://doi.org/10.1021/acs.cgd.3c00474
Cryst. Growth Des. 2023, 23, 5279−5288

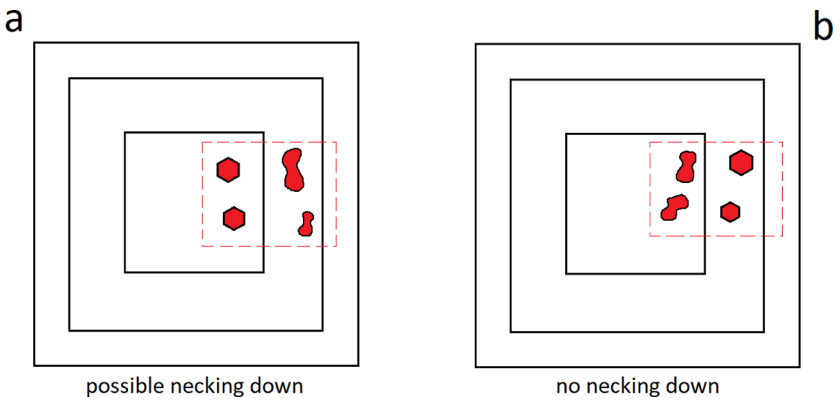

Figure 4. Schematic diagram representing two cases. (a) Inclusions with imposed morphology are closer to the central growth zone of the host phase (diamond or garnet) than those with lobed morphology: post-entrapment modification may have occurred; (b) inclusions with lobed morphology are closer to the central growth zone of the host phase (diamond or garnet) than those with imposed morphology: post-entrapment modifications cannot occur. The red dotted line marks the edge of the crystal before its resorption.

establish whether such a morphology distribution is due to post-entrapment modification or if it is syngenetic to the growth of the host i.e., a consequence of the growth and dissolution rates of the host and resorbing mineral, respectively; (2) inclusions with lobed morphology are located closer to the central growth zone of the diamond (or garnet) than those with imposed morphology (Figure 4b). In this case, it is possible to state that post-entrapment modification did not occur. Indeed, since the first inclusions to be incorporated into the host (diamond or garnet) will be those that have had more time to fix their morphology, the presence of inclusions with lobed morphology near the central growth zone cannot be explained by post-entrapment modification.

It is worth highlighting that this analysis must be done on inclusions having similar size. In fact, it is evident that small inclusions require much less mass transfer and consequently less time than larger ones to adjust their morphology.

5. CONCLUSIONS

Iso-oriented inclusions of the same phase, within a single diamond, are relicts of an original monocrystal that underwent a dissolution event during diamond growth (i.e., the inclusions are protogenetic). The processes leading to diamond-imposed versus lobed morphologies and if these processes occur during or after entrapment of the inclusion are not well-understood. To this end, we addressed the problem by initially determining the thermodynamic conditions under which two inclusions originally in contact (or one inclusion) can separate and modify their shape after trapping. Subsequently, we critically reviewed and discussed recent observations on inclusions in diamond.

The thermodynamic model we proposed to explain the post-entrapment modification showed that when strain energy exceeds a threshold value, one could obtain the separation of two inclusions originally in contact, thus increasing the S/V ratio, contrary to what is usually expected, i.e., the coarsening by crystal coalescence to minimize the surface free energies and reduce the S/V ratio. The same holds for a single inclusion: it can separate into two (or more) smaller ones only if a threshold value of strain energy is exceeded. Such unusual behavior was predicted by introducing a quadratic function to describe G_{St}, instead of a linear relationship deriving from the classic elastic theory. This different description of G_{St} deserves more in-depth analysis in the future to verify whether the hypothesized relationship is physically manifested or not. If the description we made of G_{St} is not physically supported, our thermodynamic model would exclude the separation of the inclusions, but not their morphological evolution, which is always correctly described by the Gibbs−Wulff theorem.

Although our model thermodynamically allows for post-entrapment modification of the inclusions, we do not have information about the kinetics of the process. However, it is evident that this process (separation and/or shape evolution of the inclusion) requires a significant amount of mass transfer, both from the host and inclusions, which must occur at constant volume by means of growth/dissolution processes occurring at the host/inclusion interface, coupled with grain boundary diffusion. The presence of a thin fluid film at the host/inclusion interface could facilitate the diffusion of matter and, consequently, the post-entrapment inclusion modification.

In an alternative process, the inclusion shape is being acquired during entrapment. The different morphology of the inclusions is a consequence of the growth and dissolution rates of both diamond and mineral undergoing resorption, respectively: (i) diamond-imposed morphology is due to a low diamond growth rate associated with a low dissolution rate of the reabsorbed mineral, since inclusion/diamond interfaces with the lowest interfacial energies are generated; (ii) lobed morphology is due to both the high diamond growth rate and high inclusion dissolution rate, precluding readjustment of the inclusion/diamond interface. Energetically, this mechanism should be favored with respect to that supposing the post-entrapment reshaping: the matter diffusion can take place in the presence of the fluid forming the diamond.

Based on calculations and observations reported in previous paragraphs, the maturation process of a DI after its entrapment has to be considered highly improbable. Instead, it is more reasonable to assume that during its entrapment the inclusion acquires its definitive morphology, both lobed and diamond-imposed, according to the relative growth/dissolution rates of the phases involved. We believe that the majority of mineral inclusions are protogenetic, but the imposition of diamond morphology is a syngenetic process with respect to diamond formation.

However, to obtain a definitive answer on the occurrence of the post-entrapment modification, we proposed an observational strategy, which requires a complete characterization of

https://doi.org/10.1021/acs.cgd.3c00474
Cryst. Growth Des. 2023, 23, 5279−5288

the inclusions never performed so far: morphology, crystallographic orientation, and location of the inclusions into diamond.

■ ASSOCIATED CONTENT

Supporting Information

The Supporting Information is available free of charge at https://pubs.acs.org/doi/10.1021/acs.cgd.3c00474.

Calculation of the shape coefficient and linear and quadratic G_{St} (PDF)

■ AUTHOR INFORMATION

Corresponding Author

Marco Bruno − *Dipartimento di Scienze della Terra, Università degli Studi di Torino, 10125 Torino, Italy; NIS, Centre for Nanostructured Interfaces and Surfaces, Università degli Studi di Torino, 10135 Torino, Italy;* orcid.org/0000-0002-0161-574X; Phone: +39 011 6705124; Email: marco.bruno@unito.it

Authors

Stefano Ghignone − *Dipartimento di Scienze della Terra, Università degli Studi di Torino, 10125 Torino, Italy*

Dino Aquilano − *Dipartimento di Scienze della Terra, Università degli Studi di Torino, 10125 Torino, Italy;* orcid.org/0000-0002-3908-928X

Fabrizio Nestola − *Dipartimento di Geoscienze, Università degli Studi di Padova, I-35131 Padova, Italy*

Complete contact information is available at: https://pubs.acs.org/10.1021/acs.cgd.3c00474

Notes

The authors declare no competing financial interest.

■ ACKNOWLEDGMENTS

We wish to thank both Prof. Suzette Timmerman and an anonymous reviewer for their comments, which have been useful to improve the quality of our manuscript.

■ REFERENCES

(1) Harris, J. W. The recognition of diamond inclusions. Pt. 1: Syngenetic inclusions. *Ind. Diamond Rev.* **1968**, *28*, 402.

(2) Harris, J. W. The recognition of diamond inclusions. Pt. 2: Epigenetic inclusions. *Ind. Diamond Rev.* **1968**, *28*, 458−461.

(3) Meyer, H. O. A. Inclusions in diamond. In *Mantle Xenoliths*; Nixon, P. H., Ed.; John Wiley & Sons: Chichester, 1987; pp 501−522.

(4) Nestola, F.; Nimis, P.; Angel, R. J.; Milani, S.; Bruno, M.; Prencipe, M.; Harris, J. W. Olivine with diamond-imposed morphology included in diamonds: Syngenesis or protogenesis? *Int. Geol. Rev.* **2014**, *56*, 1658−1667.

(5) Futergendler, S. I.; Frank-Kamenetsky, V. A. Oriented inclusions of olivine, garnet and chrome-spinel in diamonds. *Zapisky Vsesoyuznogo Mineralogicheskogo Obshestva* **1961**, *90*, 230−236.

(6) Sobolev, N. V. *Deep-seated Inclusions in Kimberlites and the Problem of the Composition of the Upper Mantle*; American Geophysical Union: Washington D.C, 1977.

(7) Harris, J. W.; Gurney, J. Inclusions in diamond. In *Properties of Diamond*; Field, J. E., Ed.; Academic Press: London, 1979; pp 555−591.

(8) Bulanova, G. P. The formation of diamond. *J. Geochem. Explor.* **1995**, *53*, 1−23.

(9) Pearson, D. G.; Shirey, S. B. Isotopic dating of diamonds. In *Application of Radiogenic Isotopes to ore Deposit Research and Exploration*; Lambert, D. D., Ruiz, J., Eds.; Society of Economic Geologists: Boulder, Colorado, 1999; pp 143−171.

(10) Wiggers de Vries, D. F.; Drury, M. R.; de Winter, D. A. M.; Bulanova, G. P.; Pearson, D. G.; Davies, G. R. Three-dimensional cathodoluminescence imaging and electron backscatter diffraction: Tools for studying the genetic nature of diamond inclusions. *Contrib. Mineral. Petrol.* **2011**, *161*, 565−579.

(11) Orlov, Y. L. *The Mineralogy of the Diamond*; John Wiley & Sons: New York, 1977.

(12) Taylor, L. A.; Anand, M.; Promprated, P. Diamonds and their inclusions: Are the criteria for syngenesis valid?. In *8th International Kimberlite Conference, Extended Abstract Volume; Canada*: Victoria, 2003; pp 397−402.

(13) Taylor, L. A.; Anand, M.; Promprated, P.; Floss, C.; Sobolev, N. V. The significance of mineral inclusions in large diamonds from Yakutia, Russia. *Am. Mineral.* **2003**, *88*, 912−920.

(14) Nestola, F.; Jacob, D. E.; Pamato, M. G.; Pasqualetto, L.; Oliveira, B.; Greene, S.; Perritt, S.; Chinn, I.; Milani, S.; Kueter, N.; Sgreva, N.; Nimis, P.; Secco, L.; Harris, J. W. Protogenetic garnet inclusions and the age of diamonds. *Geology* **2019**, *47*, 431−434.

(15) Pasqualetto, L.; Nestola, F.; Jacob, D. E.; Pamato, M. G.; Oliveira, B.; Perritt, S.; Chinn, I.; Nimis, P.; Milani, S.; Harris, J. W. Protogenetic clinopyroxene inclusions in diamond and Nd diffusion modeling—Implications for diamond dating. *Geology* **2022**, *50*, 1038−1042.

(16) Cesare, B.; Parisatto, M.; Mancini, L.; Peruzzo, L.; Franceschi, M.; Tacchetto, T.; Reddy, S.; Spiess, R.; Nestola, F.; Marone, F. Mineral inclusions are not immutable: Evidence of post-entrapment thermally-induced shape change of quartz in garnet. *Earth Planet. Sci. Lett.* **2021**, *555*, 116708.

(17) Roedder, E. Fluid Inclusions. *Rev. Mineral.* **1984**, *12*, 644.

(18) Lange, F. F. De-Sintering A Phenomena Concurrent with Densification Within Powder Compacts: A Review. In *Sintering Technology*; German, R. M., Messing, G. L., Cornwall, R. G., Eds.; Marcel Dekker Pubs: New York, 1996; pp 1−12.

(19) Joesten, R. Grain-Boundary Diffusion Kinetics in Silicate and Oxide Minerals. In *Advances in Physical Geochemistry*; Ganguly, J., Ed.; Springer: New York, 1991; pp 345−395.

(20) Rosenfeld, J. L.; Chase, A. B. Pressure and temperature of crystallisation from elastic effects around solid inclusions in minerals. *Am. J. Sci.* **1961**, *259*, 519−541.

(21) Zhang, Y. Mechanical and phase equilibria in inclusion−host systems. *Earth Planet. Sci. Lett.* **1998**, *157*, 209−222.

(22) Angel, R. J.; Mazzucchelli, M. L.; Alvaro, M.; Nimis, P.; Nestola, F. Geobarometry from host-inclusion systems: The role of elastic relaxation. *Am. Mineral.* **2014**, *99*, 2146−2149.

(23) Mazzucchelli, M. L.; Burnley, P.; Angel, R. J.; Morganti, S.; Domeneghetti, M. C.; Nestola, F.; Alvaro, M. Elastic geothermobarometry: Corrections for the geometry of the host-inclusion system. *Geology* **2018**, *46*, 231−234.

(24) Nye, J. F. *Physical Properties of Crystals*; Oxford Science Publications, Clarendon Press: Oxford, 1985.

(25) Angel, R. J.; Alvaro, M.; Nestola, F. Crystallographic Methods for Non-destructive Characterization of Mineral Inclusions in Diamonds. *Contrib. Mineral. Petrol.* **2022**, *88*, 257−305.

(26) Stachel, T.; Aulbach, S.; Harris, J. W. Mineral Inclusions in Lithospheric Diamonds. *Contrib. Mineral. Petrol.* **2022**, *88*, 307−391.

(27) Nestola, F.; Nimis, P.; Ziberna, L.; Longo, M.; Marzoli, A.; Harris, J. W.; Manghnani, M. H.; Fedortchouk, Y. First crystal-structure determination of olivine in diamond: Composition and implications for provenance in the Earth's mantle. *Earth Planet. Sci. Lett.* **2011**, *305*, 249−255.

(28) Mutaftschiev, B. *The Atomistic Nature in Crystal Growth*; Springer-Verlag: Berlin, 2001.

(29) Bruno, M.; Rubbo, M.; Aquilano, D.; Massaro, F. R.; Nestola, F. Diamond and its olivine inclusions: A strange relation revealed by ab initio simulations. *Earth Planet. Sci. Lett.* **2016**, *435*, 31−35.

(30) Miller, K. T.; Lange, F. F. Highly oriented thin films of cubic zirconia on sapphire through grain growth seeding. *J. Mater. Res.* **1991**, *6*, 2387−2392.
(31) Okamoto, A.; Michibayashi, K. Progressive shape evolution of a mineral inclusion under differential stress at high temperature: Example of garnet inclusions within a granulite-facies quartzite from the Lützow-Holm Complex, East Antarctica. *J. Geophys. Res.* **2005**, *110*, B11203.
(32) Nestola, F.; Jung, H.; Taylor, L. A. Mineral inclusions in diamonds may be synchronous but not syngenetic. *Nat. Commun.* **2017**, *8*, 14168.
(33) Nimis, P.; Angel, R. J.; Alvaro, M.; Nestola, F.; Harris, J. W.; Casati, N.; Marone, F. Crystallographic orientations of magnesiochromite inclusions in diamonds: What do they tell us? *Contrib. Mineral. Petrol.* **2019**, *174*, 29.
(34) Mitchell, R. S.; Giardini, A. A. Oriented olivine inclusions in diamond. *Am. Mineral.* **1953**, *38*, 136−138.
(35) Frank-Kamenetsky, V. A. The Nature of Structural Impurities and Inclusions in Minerals. Ph.D. Dissertation, University of Leningrad, Leningrad, 1964.
(36) Neuser, R. D.; Schertl, H.-P.; Logvinova, A. M.; Sobolev, N. V. An EBSD study of olivine inclusions in Siberian diamonds: Evidence for syngenetic growth? *Russ. Geol. Geophys.* **2015**, *56*, 321−329.
(37) Jacob, D. E.; Piazolo, S.; Schreiber, A.; Trimby, P. Redox-freezing and nucleation of diamond via magnetite formation in the Earth's mantle. *Nat. Commun.* **2016**, *7*, 11891.
(38) Milani, S.; Nestola, F.; Angel, R. J.; Nimis, P.; Harris, J. W. Crystallographic orientations of olivine inclusions in diamonds. *Lithos* **2016**, *265*, 312−316.
(39) Davies, G. R.; van den Heuvel, Q.; Matveev, S.; Drury, M. R.; Chinn, I. L.; Gress, M. U. A combined cathodoluminescence and electron backscatter diffraction examination of the growth relationships between Jwaneng diamonds and their eclogitic inclusions. *Mineral. Petrol.* **2018**, *112*, 231−242.
(40) Nimis, P.; Nestola, F.; Schiazza, M.; Reali, R.; Agrosì, G.; Mele, D.; Tempesta, G.; Howell, D.; Hutchison, M. T.; Spiess, R. Fe-rich ferropericlase and magnesiowüstite inclusions reflecting diamond formation rather than ambient mantle. *Geology* **2018**, *47*, 27−30.
(41) Sobolev, N. V.; Seryotkin, Y. V.; Logvinova, A. M.; Pavlushin, A. D.; Ugap'eva, S. S. Crystallographic orientation and geochemical features of mineral inclusions in diamonds. *Russ. Geol. Geophys.* **2020**, *61*, 634−649.
(42) Pamato, M. G.; Novella, D.; Jacob, D. E.; Oliveira, B.; Pearson, D. G.; Greene, S.; Afonso, J. C.; Favero, M.; Stachel, T.; Alvaro, M.; Nestola, F. Protogenetic sulfide inclusions in diamonds date the diamond formation event using Re-Os isotopes. *Geology* **2021**, *49*, 941−945.
(43) Nimis, P.; Alvaro, M.; Nestola, F.; Angel, R. J.; Marquardt, K.; Rustioni, G.; Harris, J. W.; Marone, F. First evidence of hydrous silicic fluid films around solid inclusions in gem-quality diamonds. *Lithos* **2016**, *260*, 384−389.
(44) Nestola, F.; Prencipe, M.; Nimis, P.; Sgreva, N.; Perritt, S. H.; Chinn, I. L.; Zaffiro, G. Toward a Robust Elastic Geobarometry of Kyanite Inclusions in Eclogitic Diamonds. *J. Geophys. Res.: Solid Earth* **2018**, *123*, 6411−6423.
(45) Gress, M. U.; Howell, D.; Chinn, I. L.; Speich, L.; Kohn, S. C.; van den Heuvel, Q.; Schulten, E.; Pals, A. S. M.; Davies, G. R. Episodic diamond growth beneath the Kaapvaal Craton at Jwaneng Mine, Botswana. *Mineral. Petrol.* **2018**, *112*, S219−S229.
(46) Gress, M. U.; Pearson, D. G.; Chinn, I. L.; Thomassot, E.; Davies, G. R. Mesozoic to Paleoproterozoic diamond growth beneath Botswana recorded by Re-Os ages from individual eclogitic and websteritic inclusions. *Lithos* **2021**, *388*−*389*, 106058.
(47) Gress, M. U.; Koornneef, J. M.; Thomassot, E.; Chinn, I. L.; van Zuilen, K.; Davies, G. R. Sm-Nd isochron ages coupled with C-N isotope data of eclogitic diamonds from Jwaneng, Botswana. *Geochim. Cosmochim. Acta* **2021**, *293*, 1−17.
(48) Gress, M. U.; Timmerman, S.; Chinn, I. L.; Koornneef, J. M.; Thomassot, E.; van der Valk, E. A. S.; van Zuilen, K.; Bouden, N.; Davies, G. R. Two billion years of episodic and simultaneous websteritic and eclogitic diamond formation beneath the Orapa kimberlite cluster, Botswana. *Contrib. Mineral. Petrol.* **2021**, *176*, 54.
(49) Timmerman, S.; Koornneef, J. M.; Chinn, I. L.; Davies, G. R. Dated eclogitic diamond growth zones reveal variable recycling of crustal carbon through time. *Earth Planet. Sci. Lett.* **2017**, *463*, 178−188.
(50) Timmerman, S.; Chinn, I. L.; Fisher, D.; Davies, G. R. Formation of unusual yellow Orapa diamonds. *Mineral. Petrol.* **2018**, *112*, S209−S218.
(51) Timmerman, S.; Jaques, A. L.; Weiss, Y.; Harris, J. W. N-δ^{13}C-inclusion profiles of cloudy diamonds from Koffiefontein: Evidence for formation by continuous Rayleigh fractionation and multiple fluids. *Chem. Geol.* **2018**, *483*, 31−46.

https://doi.org/10.1021/acs.cgd.3c00474
Cryst. Growth Des. 2023, 23, 5279−5288